

Determination of the $N\bar{N} \rightarrow \pi\pi$ helicity amplitudes

Geoffrey N. Epstein and Bruce H. J. McKellar

School of Physics, University of Melbourne, Parkville, Victoria, Australia 3052

(Received 6 March 1974)

General consistency conditions are derived for the $N\bar{N} \rightarrow \pi\pi$ helicity amplitudes. These are used to check previous determinations and then incorporated into a new calculation scheme to determine both s - and p -wave helicity amplitudes.

I. INTRODUCTION

The determination of the helicity amplitudes for the reaction $N\bar{N} \rightarrow \pi\pi$ has been the subject of much recent interest. These amplitudes enter the study of the relationship between πN and $\pi\pi$ scattering,¹⁻³ unitarity corrections to the extraction of the σ term for πN scattering,⁴ and the intermediate range nucleon-nucleon interaction.⁵⁻⁸ It is thus of considerable importance to determine these amplitudes accurately. The methods used in the literature use either Omnès dispersion relations,^{1,2} with the disadvantage that evaluation of the left-hand cut contribution requires extrapolation of the πN amplitude outside the ellipse of convergence of the Legendre expansion, or other analytic continuation methods which do not use our knowledge of $\pi\pi$ phase shifts. In each case it is difficult to assess the accuracy of the determination. It is our aim here to show that these problems may be overcome and accurate helicity amplitudes obtained by use of helicity-amplitude consistency conditions.

In Sec. II we sketch the Omnès dispersion relation approach to evaluating $N\bar{N} \rightarrow \pi\pi$ helicity amplitudes and identify the input required for accurate solutions. Then in Sec. III we give a short account of the $\pi\pi$ interaction. In Sec. IV we present a derivation of helicity-amplitude consistency conditions which are initially used as checks on previous helicity-amplitude determinations, and then in later sections incorporated into a new helicity-amplitude calculational scheme. In particular, in Sec. V we use a novel form of Omnès dispersion relation to evaluate f_+^0 , and then in Sec. VI demonstrate the efficacy of using non-Born dispersion relations to evaluate f_-^1 and Γ_2 , where

$$\Gamma_2 = (f_+^1 - m f_-^1 / \sqrt{2}) [2/m^2 - \frac{1}{4}t]^{-1}$$

(we use units such that $\hbar = c = m_\pi = 1$, the metric $ds^2 = \vec{dx}^2 - dt^2$, and the notation m for the nucleon mass). Γ_2 is evaluated directly instead of being calculated from f_+^1 and f_-^1 because it appears in the calculation of the nucleon-nucleon potential.⁶⁻⁸ The actual evaluations of f_-^1, Γ_2 are detailed in

Sec. VII; in each case the calculated amplitudes are compared with previous works and a careful estimate of errors made. Section VIII summarizes our results, a preliminary account of which has appeared elsewhere.⁹

II. OMNÈS DISPERSION RELATIONS

To write down dispersion relations for the helicity amplitudes $f_\pm^J(t)$ we need to know the appropriate analytic properties. These were first deduced by Frazer and Fulco¹⁰ using the Mandelstam representation for A^\pm, B^\pm and the helicity amplitude projection formulas. The principal features are two branch cuts: one from $t = -\infty$ to $4(1 - 1/4m^2)$ and the other from $t = 4$ to ∞ . There are no kinematical singularities. In addition, unitarity places bounds on the asymptotic behavior as $t \rightarrow \infty$, so that at worst

$$\begin{aligned} f_+^J(t) &\sim t^{-J+1/2}, \\ f_-^J(t) &\sim t^{-J}. \end{aligned} \quad (2.1)$$

Thus we can write for $J \neq 0$

$$\begin{aligned} f_\pm^J(t) = &\frac{1}{\pi} \int_{-\infty}^a dt' \frac{\text{Im} f_\pm^J(t')}{t' - t - i\epsilon} \\ &+ \frac{1}{\pi} \int_4^\infty dt' \frac{\text{Im} f_\pm^J(t')}{t' - t - i\epsilon}, \end{aligned} \quad (2.2)$$

where

$$a = 4 \left(1 - \frac{1}{4m^2} \right).$$

For $J=0$, $f_-^0(t)=0$, so we are left with $f_+^0(t)$, which requires one subtraction. [In principle, one could subtract at $t=4m^2$ since $f_+^0(4m^2)=0$; however, in practice this is of little use due to the slow convergence of the dispersion integrals.]

Relation (2.2) presents two problems. The first is that there is no straightforward way to evaluate the right-hand (RH) cut, and the second is that at best we only know the left-hand (LH) cut in the range $-26 < t < a$. This latter circumstance arises because we determine $\text{Im} f_\pm^J$ on the LH cut by using a Legendre extrapolation from the physical πN

scattering region. To be explicit we write down the appropriate equations¹⁰:

$$\begin{aligned} \text{Im}f_+^J &= -\frac{1}{8\pi(p_-q_-)^J} \left\{ \pi g^2 m z_0 P_J(z_0) + \theta(-t) \int_{(m+1)^2}^{L(t)} ds' \left[\left(\frac{p_-}{q_-} \right) a_1(s', t) + m z b_1(s', t) \right] P_J(z) \right\}, \\ \text{Im}f_-^J &= \frac{[J(J+1)]^{1/2}}{8\pi(2J+1)(p_-q_-)^J} \left\{ \pi g^2 [P_{J+1}(z_0) - P_{J-1}(z_0)] + \theta(-t) \int_{(m+1)^2}^{L(t)} ds' b_1(s', t) [P_{J+1}(z) - P_{J-1}(z)] \right\}, \end{aligned} \quad (2.3)$$

where

$$\begin{aligned} z_0 &= (m^2 - p_-^2 - q_-^2) / 2p_-q_-, \\ z &= (s' - p_-^2 - q_-^2) / 2p_-q_-, \\ L(t) &= m^2 + 1 + 2p_-q_- - \frac{1}{2}t, \\ p_-^2 &= m^2 - \frac{1}{4}t, \\ q_-^2 &= 1 - \frac{1}{4}t, \end{aligned} \quad (2.4)$$

and we note that

$$\begin{aligned} a_1^\pm(s', t) &= \text{Im}A^\pm(s', t), \\ b_1^\pm(s', t) &= \text{Im}B^\pm(s', t), \quad \text{for } t < 0. \end{aligned} \quad (2.5)$$

Now we can see that the Legendre extrapolation of a_1, b_1 is required because the upper integration limit $L(t)$ requires $\cos\theta < -1$, where θ is the πN scattering angle. As usual, the Legendre extrapolation is hemmed in by the nearest singularities, which in this case occur at $t \simeq -4m$, i.e., $t \simeq -26$.

Fortunately, we can overcome both of the above problems by employing Omnès dispersion relations subtracted to reduce the importance of the unknown distant cuts. To derive these relations¹⁰ the key step is to observe that t -channel unitarity says

$$\text{Im}f_\pm^J(t) = f_\pm^J(t)^* e^{i\delta_J^I} \sin\delta_J^I, \quad \text{for } 4 < t < 16. \quad (2.6)$$

δ_J^I is the $\pi\pi$ phase shift in the state of angular momentum J and isospin I . We observe that since we are dealing with the $N\bar{N} \rightarrow \pi\pi$ reaction the isospin must be 0 or 1. Thus in relation (2.6) the statistics imply that

$$J \text{ even} \rightarrow I = 0, \quad (2.7)$$

$$J \text{ odd} \rightarrow I = 1.$$

Now we define

$$\mu_J(t) = \frac{t}{\pi} \int_4^\infty dt' \frac{\delta_J^I(t')}{t'(t' - t - i\epsilon)} \quad (2.8)$$

and consider the function $f_\pm^J(t) e^{-\mu_J(t)}$, which is real in the interval $4 < t < 16$. The appropriate dispersion relation is

$$\begin{aligned} f_\pm^J(t) e^{-\mu_J(t)} &= \frac{1}{\pi} \int_{-\infty}^a dt' \frac{e^{-\mu_J(t')}}{t' - t - i\epsilon} \text{Im}f_\pm^J(t') \\ &\quad + \frac{1}{\pi} \int_{16}^\infty dt' \frac{\text{Im}[f_\pm^J(t') e^{-\mu_J(t')}]}{t' - t - i\epsilon}. \end{aligned} \quad (2.9)$$

Next we neglect the RH-cut integral. This approximation is strengthened by the fact that in practice the unitarity relation (2.6) holds up to $t = 50$ at least for s - and p -wave $\pi\pi$ interactions.¹¹ In addition, if we subtract the dispersion relation, we reduce the distant cut contribution for *both* cuts, so not only do we reduce the known LH-cut contribution, but we also further increase the accuracy of the "exact" unitarity approximation.

It is clear now that to implement this subtracted Omnès dispersion relation scheme, we need to know the appropriate $\pi\pi$ phase shifts and subtraction constants.

III. $\pi\pi$ PHASE SHIFTS

The $\pi\pi$ interaction offers considerable problems for the experimentalist and much effort has been directed at its elucidation. Our aim here is to indicate what we consider to be the "best" $\pi\pi$ phase shifts for input to our dispersion relations. For a more complete coverage we refer the reader to the excellent reviews of Jackson,¹² Morgan and Pišút,¹³ and Petersen,¹⁴ together with the recent papers by Basdevant *et al.*¹⁵

From an experimental point of view the most important feature of the $\pi\pi$ interaction is that it cannot be studied directly at present. The short lifetime of the pions forces the study of reactions in which the final state is generated by a $\pi\pi$ vertex. To counterbalance these difficulties the $\pi\pi$ system offers some simplifying features. In particular it turns out that up to 1 GeV ($t \sim 50$), $\pi\pi$ scattering is well described by s , p , and d waves. Thus we have the phase shifts $\delta_0^0, \delta_2^0, \delta_1^1, \delta_2^1, \delta_2^2$ (notation δ_J^I). This simple description applies because the pion has spin zero, the forces are of short range, $\pi\pi \neq 3\pi$ because of G parity, and $\pi\pi \rightarrow 4\pi$ appears only at high energies. Since we are interested here in the amplitude $N\bar{N} \rightarrow \pi\pi$ we can forget those $\pi\pi$ waves with isospin different from 0 or 1. In addition δ_2^0 is very small and is neglected in our subsequent analysis. Thus we are left with δ_0^0 and δ_1^1 .

The extraction of δ_0^0 has been a major problem. However, our current picture of the $\pi\pi$ s wave is fairly clear due to the accumulation of much experimental data and the analyses of Morgan and Shaw¹⁶ and, more recently, Basdevant *et al.*¹⁵ It

now appears that the best available solution is of the between-down/down form. We show this δ_0^0 in Fig. 1 [for a parametrization see Appendix A]. Above 900 MeV δ_0^0 rises rapidly and appears to flatten off on reaching π . The low-energy behavior of δ_0^0 is also of interest and it appears that experimental estimates of the scattering length are converging on the original soft-pion result of Weinberg,¹⁷ i.e., $a_0 = 0.2$.

Now we turn to the p -wave $\pi\pi$ phase shift δ_1^1 . The fact that this is resonant at about 760 MeV has been known for some time. Also the scattering length is reasonably well established as

$$a = 0.035 \pm 0.005. \quad (3.1)$$

However, there is still some uncertainty about the width of the resonance. The current favored value is

$$\Gamma_\rho = (135 \pm 15) \text{ MeV}, \quad (3.2)$$

compared with the older value of 120 MeV. It is interesting to note that electron-positron annihilation to two pions and pion electroproduction give information on the pion electromagnetic form factor

$$F_\pi(t) = e^{\mu_1(t)} \quad (3.3)$$

for spacelike (+ve) and timelike (-ve) t , respectively. Thus it would appear that the most straightforward procedure would be to put the experimental values for $F_\pi(t)$ directly into our Omnès dispersion relations for f_-^1, Γ_2 . However, the data are not as accurate as one would wish. In Fig. 2 we plot the pion electroproduction data of Akerlof *et al.*,¹⁸ Mistretta *et al.*,¹⁹ and Brown *et al.*,²⁰ together with the Novosibirsk electron-positron annihilation data of Auslender *et al.*²¹ It is im-

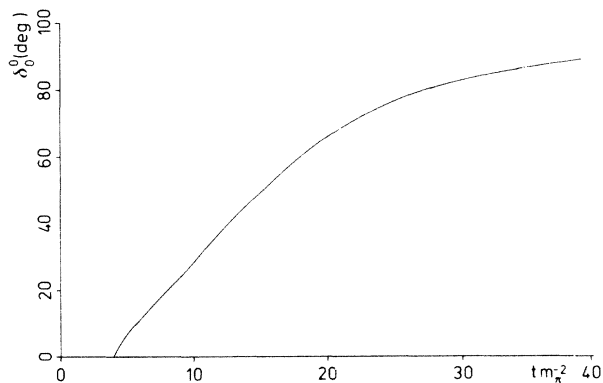


FIG. 1. The $\pi\pi$ phase shift δ_0^0 .

portant to note that these experimental results are model-dependent. This is particularly true of the electroproduction data. The Akerlof *et al.* and Mistretta *et al.* error bars are meant to include both theoretical and statistical errors, while those of Brown are purely statistical. The Novosibirsk electron-positron data quoted here have a "model dependence" caused by the treatment of the ρ - ω interference. Auslender *et al.* employ a crude model and give a value 105 MeV for the ρ width. More recent Orsay data²² indicate a larger width, and when the raw Novosibirsk data are combined with this and a realistic model employed for ρ - ω interference a width of 135 MeV is obtained. (The Orsay data are not given in a form readily amenable to plotting.) In view of this we feel that the best approach is to work from the δ_1^1 phase shift.

We use $\Gamma_\rho = 135$ MeV and parametrize the phase as in Morgan and Shaw¹⁶ (see Appendix A). The phase shifts for the present width of 135 MeV are shown in Fig. 3 where we show the older 120-MeV width set for comparison. We have plotted the corresponding curves (labeled A, B) for $|F_\pi(t)|$ in Fig. 2. One of the interesting features is that $F_\pi(t)$ for $t < 0$ is independent of the ρ width and is consistent with the most recent electroproduction analysis (Brown *et al.*)²⁰ We emphasize that it is important to include the high-energy δ_1^1 contribution. In the spirit of Pišút and Roos²³ we have used $\delta_1^1 = \pi$ for $t > 100$. For comparison we have also plotted (curve C) in Fig. 2 the results

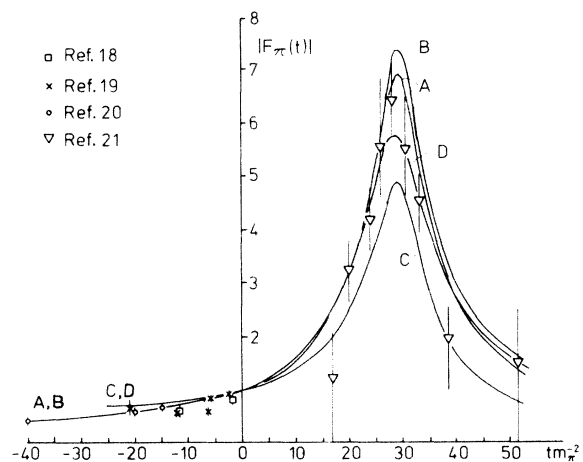


FIG. 2. Plot of $|F_\pi(t)|$ vs t . Curve A is drawn for a ρ width of 135 MeV, and curve B is for a ρ width of 120 MeV. Curve C corresponds to a width of 135 MeV, but with the high-energy tail of the $\pi\pi$ interaction omitted. Curve D is another possible fit to the data.

obtained if we arbitrarily set δ_1^1 to zero for $t > 100$ for the 135-MeV phase shift. We make the point, however, that although we must include the high-energy tail, the results for $|F_\pi(t)|$ are insensitive to any reasonable variations of detail. We also draw in another curve (D), which we use later to obtain an estimate of the accuracy of our determinations of f_-^1, Γ_2 .

Thus we have chosen the $\pi\pi$ phase shifts for use in our Omnès dispersion relations. The remaining problem is to evaluate dispersion-relation subtraction constants. Our principal tool here is a set of helicity-amplitude consistency conditions which we derive in Sec. IV.

IV. HELICITY-AMPLITUDE CONSISTENCY CONDITIONS

Our consistency conditions constrain the helicity amplitudes at $t=4$ and are derived simply by observing that in the usual integrals over the πN center-of-mass energy of the πN invariant amplitudes, projecting out the $N\bar{N} \rightarrow \pi\pi$ helicity amplitudes, the range of integration collapses at the $\pi\pi$ threshold to a single point. Thus at the $\pi\pi$ threshold the helicity amplitudes are given directly in terms of the unphysical s -channel invariant amplitudes.

To begin with, we write down general projection formulas for $f_\pm^J(t)$. For J even,

$$f_+^J(t) = \frac{m(m^2 - \frac{1}{4}t)}{8\pi(pq)^{J+1}} \int_{-pq/m}^{pq/m} d\nu P_J\left(\frac{m\nu}{pq}\right) C^+(\nu, t), \quad (4.1a)$$

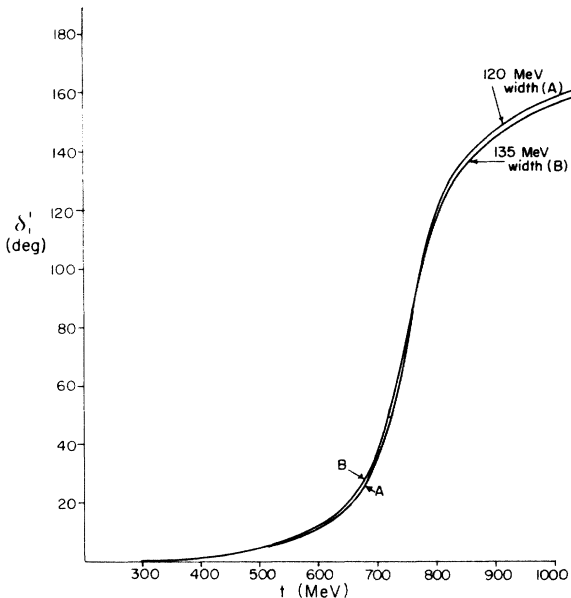


FIG. 3. The $\pi\pi$ phase shift δ_1^1 .

$$f_-^J(t) = \frac{m[J(J+1)]^{1/2}}{8\pi(2J+1)(pq)^J} \times \int_{-pq/m}^{pq/m} d\nu \left[P_{J-1}\left(\frac{m\nu}{pq}\right) - P_{J+1}\left(\frac{m\nu}{pq}\right) \right] \times B^+(\nu, t), \quad (4.1b)$$

and for J odd,

$$f_+^J(t) = \frac{m(m^2 - \frac{1}{4}t)}{8\pi(pq)^{J+1}} \int_{-pq/m}^{pq/m} d\nu P_J\left(\frac{m\nu}{pq}\right) C^-(\nu, t), \quad (4.1c)$$

$$f_-^J(t) = \frac{m[J(J+1)]^{1/2}}{8\pi(2J+1)(pq)^J} \times \int_{-pq/m}^{pq/m} d\nu \left[P_{J-1}\left(\frac{m\nu}{pq}\right) - P_{J+1}\left(\frac{m\nu}{pq}\right) \right] \times B^-(\nu, t), \quad (4.1d)$$

where

$$\nu = \frac{pq}{m} \cos\phi = \frac{s - \mu}{4m},$$

ϕ = center-of-mass $N\bar{N} \rightarrow \pi\pi$ scattering angle

and

$$C^\pm(\nu, t) = A^\pm(\nu, t) + \frac{\nu}{1 - t/4m^2} B^\pm(\nu, t).$$

Now we set $t=4$ (which implies $q \rightarrow 0$) and obtain our consistency conditions. To be explicit we now restrict our attention to the $J=0, 1$ helicity amplitudes, for which we find

$$\text{Re}f_+^0(4) = \frac{m^2 - 1}{4\pi} A^+(0, 4), \quad (4.2a)$$

$$\text{Re}f_-^1(4) = \frac{B^-(0, 4)\sqrt{2}}{12\pi}, \quad (4.2b)$$

$$\text{Re}\Gamma_2(4) = \frac{1}{24\pi m} \left[\frac{\partial A^-(\nu, 4)}{\partial \nu} \right]_{\nu=0} \quad (4.2c)$$

Evaluating the right-hand-side expressions using the results of Engels²⁴ and Höhler and Strauss²⁵ together with the πN amplitude tables of Nielsen,²⁶ we obtain

$$\text{Re}f_+^0(4) = 110.0 \pm 0.5, \quad (4.3a)$$

$$\text{Re}\tilde{f}_-^1(4) = 0.35 \pm 0.01, \quad (4.3b)$$

$$\text{Re}\Gamma_2(4) = 0.019 \pm 0.001, \quad (4.3c)$$

where we use the standard decomposition

$$f_\pm^1 = f_\pm^1|_{\text{Born}} + \tilde{f}_\pm^1. \quad (4.4)$$

Explicitly, $f_\pm^J(t)|_{\text{Born}}$ is obtained by inserting the nonintegral terms in Eq. (2.3) for $g_m f_\pm^J$ into the left-hand cut of the dispersion relation (2.2).

As an initial application of these relations we test published helicity-amplitude determinations.

In particular we note that for the $J=0$ amplitude Nielsen, Petersen, and Pietarinen³ obtained $f_+^0(4) \sim 55$, a factor of two smaller than required by (4.3a). However, we find the $J=1$ results of Höhler, Strauss, and Wunder (HSW),

$$\begin{aligned} \text{Re}\tilde{f}_-^1(4)|_{\text{HSW}} &= 0.25, \\ \text{Re}\Gamma_2(4)|_{\text{HSW}} &= 0.016, \end{aligned} \quad (4.5)$$

are in fair agreement with our values.

In the next few sections we develop a calculational scheme based on the consistency conditions and Omnès dispersion relations for the helicity amplitudes. As stated earlier, one of the major problems has been to estimate the contribution of the unknown distant LH cut ($-\infty < t < -26$). Since we now have a good value of the amplitude at $t=4$ we can either use this directly as a subtraction constant to reduce the importance of the unknown distant LH cut or, if more convenient, we can subtract at some other point and adjust the subtraction constant to force the amplitude to obey our consistency condition. In practice we find that to attain the necessary accuracy we need to subtract twice, so we require the value of the second

subtraction constant, too. For f_+^0 we can use results from forward πN scattering data to evaluate one of the subtraction constants reliably, so we have no problems there. However, the same technique is not accurate enough for f_-^1, Γ_2 . Fortunately, our consistency conditions provide a method for obtaining an estimate of the other subtraction constant. Since our approaches for f_+^0 and f_-^1, Γ_2 are quite different, we treat them separately in the following sections.

V. THE f_+^0 DISPERSION RELATION

To preface this section we remark that previous determinations of f_+^0 are very crude except for the very recent work of Nielsen and Oades² which we discuss below. In particular, the results of Hamilton *et al.*,²⁷ and more recently Nielsen, Petersen, and Pietarinen³ appear to be only qualitatively correct. They fail our consistency condition test by a large margin (see Sec. IV). In view of this and the recent reliable determination of δ_0^0 we attempt a new, accurate evaluation of f_+^0 .

The dispersion relation we use for f_+^0 is twice subtracted at $t=0$ and has the form

$$\begin{aligned} e^{-\mu_0(t)}f_+^0(t) &= \text{Re}f_+^0(0) + t \left[\frac{\partial}{\partial t} \text{Re}[e^{-\mu_0(t)}f_+^0(t)] \right]_{t=0} + \frac{\text{Im}f_+^0(0)}{\pi} \left\{ \ln \left[\frac{26(t-a)}{a(t+26)} \right] + t \left(\frac{1}{a} + \frac{1}{26} \right) \right\} \\ &+ \frac{t}{\pi} \left[\frac{\partial}{\partial t} \text{Im}[e^{-\mu_0(t)}f_+^0(t)] \right]_{t=0} \ln \left[\frac{26(t-a)}{a(t+26)} \right] \\ &+ \frac{t^2}{\pi} \int_{-26}^a dt' \frac{e^{-\mu_0(t')} \text{Im}f_+^0(t') - \text{Im}f_+^0(0) - t' \left\{ (\partial/\partial t'') \text{Im}[e^{-\mu_0(t'')}f_+^0(t'')] \right\}_{t''=0}}{(t'-t)(t')^2}, \quad \text{for } t > 4. \end{aligned} \quad (5.1)$$

This relation is different from the usual one used by Hamilton and others,²⁷ namely

$$e^{-\mu_0(t)}f_+^0(t) = \text{Re}f_+^0(0) + t \left[\frac{\partial}{\partial t'} \text{Re}[e^{-\mu_0(t')}f_+^0(t')] \right]_{t'=0} + \frac{t^2}{\pi} \left[\frac{\partial}{\partial t''} \left(\text{P} \int_{-26}^a dt' \frac{e^{-\mu_0(t')} \text{Im}f_+^0(t')}{(t'-t'')(t'-t)} \right) \right]_{t''=0}. \quad (5.2)$$

We include a derivation of (5.1) in Appendix B. Its principal advantage is that numerical evaluation is much simpler, for the limiting procedures required by the Hamilton relation are avoided. We have checked the numerical accuracy of our relation by using the same input as was used by Hamilton *et al.*²⁷ in 1962 and we reproduce exactly the Hamilton $\text{Im}f_+^0$. Also, if we input the phase-shift predictions of NPP we get their results for $\text{Im}f_+^0$.

In practice we find that the two subtractions lead to a highly convergent relation. (We note that just one subtraction gives poor accuracy.) The LH-cut contribution is rapidly reduced at large negative t and in our evaluation the Born term gives the dominant (>95%) LH-cut contribution [we use the Nielsen tables²⁸ for $\text{Im}\tilde{f}_+^0(t)$]. As stated earlier we, employ as input the Morgan and Shaw-type δ_0^0 and we find that f_+^0 is not sensi-

tive to the experimental errors¹⁵ attached to δ_0^0 . The main problem is that the solution for f_+^0 is sensitive to the derivative subtraction constant. Early analysis of forward πN scattering by Menotti²⁸ yielded the values

$$\text{Re}f_+^0(0) = -1.9 \pm 3.0, \quad (5.3a)$$

$$\frac{\partial}{\partial t} \text{Re}f_+^0(t) \Big|_{t=0} = 2.8 \pm 0.9. \quad (5.3b)$$

We have found that (5.3b) is not accurate enough for our purposes. However, we can evaluate the derivative subtraction constant in the following way. We use a recent determination for the first subtraction constant,²⁹ i.e.,

$$\text{Re}f_+^0(0) = -2.8 \pm 0.7, \quad (5.4)$$

together with the Morgan and Shaw phase shift as

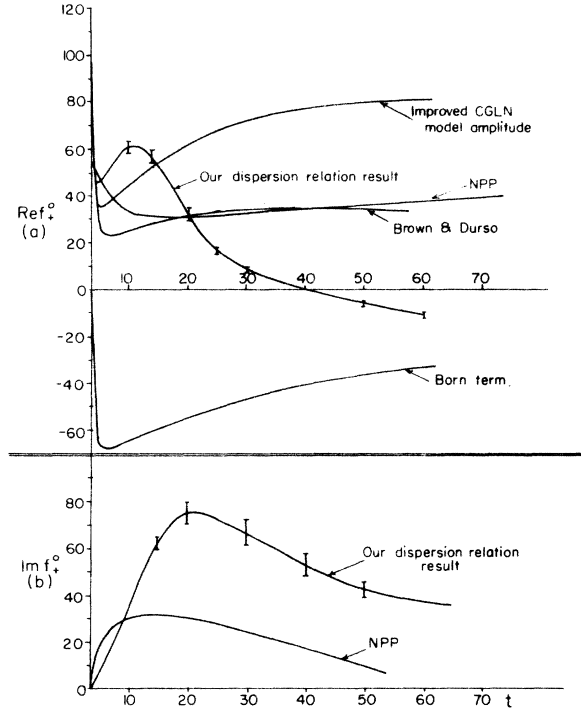


FIG. 4. (a) Real and (b) imaginary parts of the f_+^0 amplitude.

input to our dispersion relation evaluated at $t=4$. By imposing the f_+^0 consistency condition we find

$$\left. \frac{\partial}{\partial t} \text{Re} f_+^0(t) \right|_{t=0} = 2.0 \pm 0.2. \quad (5.5)$$

We note that the determination is quite insensitive to the value of $\text{Re} f_+^0(0)$. It is interesting to note that the subtraction constants may be determined in a quite different way. This entails use of the improved accurate CGLN model for the πN amplitude, which we have derived and explained in detail elsewhere.⁸ With this model we predict

$$\begin{aligned} \text{Re} f_+^0(0) \Big|_{\text{CGLN}} &= -2.0, \\ \left. \frac{\partial}{\partial t} \text{Re} f_+^0(t) \right|_{\text{CGLN}, t=0} &= 1.8. \end{aligned} \quad (5.6)$$

We now turn to our results for f_+^0 . We show both $\text{Re} f_+^0$ and $\text{Im} f_+^0$ in Figs. 4(a) and 4(b) with error bars indicating the spread corresponding to the uncertainty in the derivative subtraction constant. For comparison we have drawn in the "improved" CGLN model prediction for $\text{Re} f_+^0$

together with the Born contribution alone. We have also plotted the results of Nielsen, Petersen, and Pietarinen (NPP)³ and Brown and Durso³⁰ which were used in the recent NN interaction calculations of Brown and Durso,³⁰ Chemtob and Riska³¹ and Chemtob, Durso, and Riska.⁷

It is clear from the comparison that the accuracy of previous determinations is poor. From the CGLN model f_+^0 we can also understand why Kapadia³² had cutoff problems in evaluating the corresponding NN potential integrals. We also note for later reference that the Born term is large and responsible for the rapid variations in f_+^0 near $t=4$.

We should also mention the recent work of Nielsen and Oades,² which provides an evaluation of f_+^0 which has an accuracy comparable to that of the present work. They use unsubtracted dispersion relations and attempt an extrapolation of the distant LH-cut contribution from the region $t < a$ to the region of interest $t > 4$. Results are given for $\text{Im} f_+^0$ only. It is clear at this point that with the NO phase-shift input our f_+^0 coincides with the NO f_+^0 .

VI. NON-BORN DISPERSION RELATIONS

So far we have used Omnès dispersion relations to calculate the complete helicity amplitudes. However, we already know the Born amplitudes so it is natural to ask the question: Why not concentrate on accurately evaluating that part of the amplitude which we do not know, i.e., the non-Born part? This approach appears particularly attractive in relation to evaluations of the NN potential, for there the g^4 terms of the helicity-amplitude expansion are subtracted out leaving the smaller (non-Born)² and (non-Born \times g^2) cross terms.⁸ We shall also find in Sec. VII that non-Born dispersion relations are essential if we are to implement our consistency conditions directly.

We observe that non-Born dispersion relations have advantages which appear not to have been exploited in previous amplitude determinations. For this reason we briefly derive and discuss these relations. First we write

$$f_{\pm}^J(t) = f_{\pm}^J(t) \Big|_{\text{Born}} + \tilde{f}_{\pm}^J(t) \quad (6.1)$$

and observe that $f_{\pm}^J(t)$ has a LH cut from $t=0$ to $-\infty$ and a RH cut from $t=4$ to ∞ . Thus we have

$$f_{\pm}^J(t) e^{-\mu_J(t)} = \frac{1}{\pi} \int_{-\infty}^0 dt' \frac{e^{-\mu_J(t')}}{t' - t - i\epsilon} \text{Im} \tilde{f}_{\pm}^J(t') + \frac{1}{\pi} \int_4^{\infty} dt' \frac{\text{Im} \{ [f_{\pm}^J(t') - f_{\pm}^J(t') \Big|_{\text{Born}}] e^{-\mu_J(t')} \}}{t' - t - i\epsilon}. \quad (6.2)$$

Then if we apply unitarity in the usual way, we arrive at our non-Born dispersion relation

$$\begin{aligned} \bar{f}_\pm^J(t)e^{-\mu_J(t)} &= \frac{1}{\pi} \int_{-\infty}^0 dt' \frac{e^{-\mu_J(t')} \text{Im} \bar{f}_\pm^J(t')}{t' - t - i\epsilon} \\ &+ \frac{1}{\pi} \int_4^\infty dt' \frac{f_\pm^J(t')|_{\text{Born}} \sin \delta_J^I(t')}{e^{\mu_J(t')} (t' - t - i\epsilon)}. \end{aligned} \quad (6.3)$$

The advantages of this relation are apparent. First of all, the unknown (non-Born) distant LH-cut contribution is neatly isolated and the Born terms appear on the RH-cut, where their contribution is certainly more accurately evaluated than if they appeared on the distant LH cut. As a result of these features the relation is particularly suited for approaches such as that of Nielsen and Oades² in which the unknown LH cut is extrapolated.

In Sec. VII we evaluate f_-^1, Γ_2 using non-Born dispersion relations subtracted at threshold ($t=4$) and at resonance ($t \sim 30$). We also show how the resonance subtraction constants may be estimated using unsubtracted non-Born dispersion relations together with our consistency conditions.

VII. THE f_-^1, Γ_2 DISPERSION RELATIONS

Previous attempts³³ to calculate the $J=1$ helicity amplitudes employed Omnès dispersion relations twice subtracted at $t=0$ following the approach used for the f_+^0 amplitude. However, this method is inaccurate for the $J=1$ amplitudes. To illustrate the difficulty we consider the Omnès relation for f_-^1 (the Γ_2 case is entirely analogous). We have

$$\begin{aligned} f_-^1(t) &= e^{\mu_1(t)} \text{Re} f_-^1(0) \\ &+ e^{\mu_1(t)} t \left[\frac{\partial}{\partial t'} \text{Re} f_-^1(t') \right]_{t'=0} \\ &+ \text{other terms.} \end{aligned} \quad (7.1)$$

From this it is clear that at resonance the derivative subtraction constant error will be magnified by a factor of about 200. Using the results of Vick,³³ namely

$$\begin{aligned} \left. \frac{\partial}{\partial t} \text{Re} f_-^1(t) \right|_{t=0} &= -0.053 \pm 0.007, \\ \left. \frac{\partial}{\partial t} \text{Re} \Gamma_2(t) \right|_{t=0} &= -0.00582 \pm 0.00025, \end{aligned} \quad (7.2)$$

$$\begin{aligned} \bar{f}_\pm^1(t)e^{-\mu_1(t)} &= \frac{t-t_\rho}{4-t_\rho} \text{Re} \bar{f}_\pm^1(4)e^{-\mu_1(4)} + \frac{t-4}{t_\rho-4} \text{Im} \bar{f}_\pm^1(t_\rho) |e^{-\mu_1(t_\rho)}| \\ &+ \frac{(t-4)(t-t_\rho)}{\pi} \left\{ \int_{-\infty}^0 dt' \frac{e^{-\mu_1(t')} \text{Im} \bar{f}_\pm^1(t')}{(t'-4)(t'-t_\rho)(t'-t)} + \text{P} \int_4^\infty dt' \frac{f_\pm^1(t')|_{\text{Born}} \sin \delta_1^1(t')}{|e^{\mu_1(t')}| (t'-4)(t'-t_\rho)(t'-t)} \right\} \end{aligned} \quad \text{for } t > 4, \quad (7.5)$$

we find that the corresponding resonance errors are

$$\begin{aligned} \text{Error} \{f_-^1(30)\} &\sim 1.4, \\ \text{Error} \{\Gamma_2(30)\} &\sim 0.05. \end{aligned} \quad (7.3)$$

These errors are of the same order of magnitude as the amplitudes (this is in marked contrast to the f_+^0 case, where the corresponding errors are typically 5% of the amplitude). Thus subtracting twice at $t=0$ is out of the question.

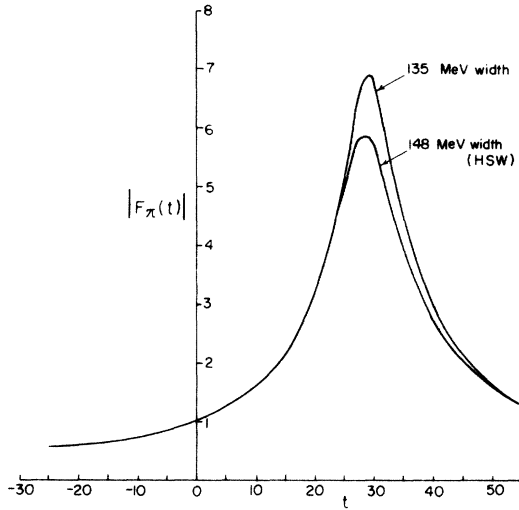
The later work of Hühler, Strauss, and Wunder (HSW)¹ used subtractions at $t=0$ and $t=-20$, e.g.,

$$\begin{aligned} f_-^1(t) &= e^{\mu_1(t)} \left[\frac{1}{20}(t+20) \right] \text{Re} f_-^1(0) \\ &- e^{\mu_1(t)} \left(\frac{1}{20}t \right) \text{Re} f_-^1(-20) e^{\mu_1(-20)} \\ &+ \text{other terms.} \end{aligned} \quad (7.4)$$

Thus, the HSW work is more accurate as the error magnification at resonance is smaller (~ 20). However, a $\pi\pi$ p -wave phase shift of width 148 MeV was used (as compared with the current value of 135 MeV). In addition, the HSW amplitudes do not quite satisfy our consistency conditions. We remark that HSW actually determined f_\pm^1 whereas we calculate the amplitudes f_-^1 and Γ_2 , for these are the quantities directly entering the NN calculation, and we observe that calculating Γ_2 from f_\pm^1 can lead to large errors (up to 25% at the resonance).

In view of the above we attempt a new derivation of f_-^1, Γ_2 . We emphasize that the NN potential is very sensitive to the $J=1$ amplitudes,⁸ so it is most important to know these amplitudes as accurately as possible.

We feel that the best approach is to use Omnès dispersion relations subtracted at $t=4$ and at resonance. This allows direct use of our consistency conditions but requires an evaluation of the resonance amplitudes. In addition, we have found particularly for f_-^1 that the subtraction at $t=4$ in the full amplitude dispersion relation causes sensitivity to the value of $F_\pi(t)$ at $t \approx 4$. The reason for this is that the Born term on the LH cut varies extremely rapidly near $t=a$ (see Appendix C). If non-Born dispersion relations are used, this problem disappears. Thus we use

FIG. 5. $|F_\pi(t)|$. Comparison of HSW result with ours.

where $t_\rho = 29.8$.

A similar relation holds for $\tilde{\Gamma}_2(t)$. The main problem now is to evaluate $\text{Im}\tilde{f}_-^1(t_\rho)$ and $\text{Im}\tilde{\Gamma}_2(t_\rho)$. It is instructive here to look back at the HSW paper. In particular we show in Fig. 5 the HSW $F_\pi(t)$ input together with ours. The striking feature here is that the two curves coincide up to the resonance region. We also find that the HSW values of \tilde{f}_-^1 in the region $t < 0$ compare well with the recent accurate values of Nielsen.²⁶

In view of the above results it is reasonably clear that the principal difference between the HSW results and ours will be due to the change in $F_\pi(t)$ near resonance. [We note here the subtle point that $|F_\pi(t)|$ peaks at $t \sim 29$, i.e., about 10 MeV below resonance. This behavior was also found by Gounaris and Sakurai.³⁴] The HSW resonance amplitudes are

$$\text{Im}\tilde{f}_-^1(t_\rho)|_{\text{HSW}} \approx 1.27, \quad (7.6)$$

$$\text{Im}\tilde{f}_+^1(t_\rho)|_{\text{HSW}} \approx 1.9,$$

which imply that $\text{Im}\tilde{\Gamma}_2(t_\rho)|_{\text{HSW}} \approx -0.053$, but we remind the reader that a 5% error in f_-^1 here implies a 25% error in Γ_2 , so the HSW values of Γ_2 are not very accurate. Using our 135-MeV width δ_1^1 for $F_\pi(t)$ (i.e., curve A of Fig. 2, see Sec. III), we find that these values are altered to

$$\text{Im}\tilde{f}_-^1(t_\rho) \approx 1.5, \quad (7.7)$$

$$\text{Im}\tilde{\Gamma}_2(t_\rho) \approx -0.063,$$

where again the \tilde{f}_-^1 value is the more accurately determined. We can make an independent check on these amplitudes by using unsubtracted non-Born dispersion relations together with our consistency conditions. At this point we merely quote the

results, leaving the details till the end of the section. We find that there is quite some latitude in the choice of subtraction constants. The consistency condition limits are

$$0.97 < \text{Im}\tilde{f}_-^1(t_\rho) < 1.48$$

and

$$-0.1 < \text{Im}\tilde{\Gamma}_2(t_\rho) < -0.051. \quad (7.8)$$

Faced with this situation we can make some consistent subtraction-constant choice and plot the resulting f_-^1, Γ_2 amplitudes calculated from (7.5) with error bars indicating the spread of solutions allowed by the consistency conditions. We choose the set

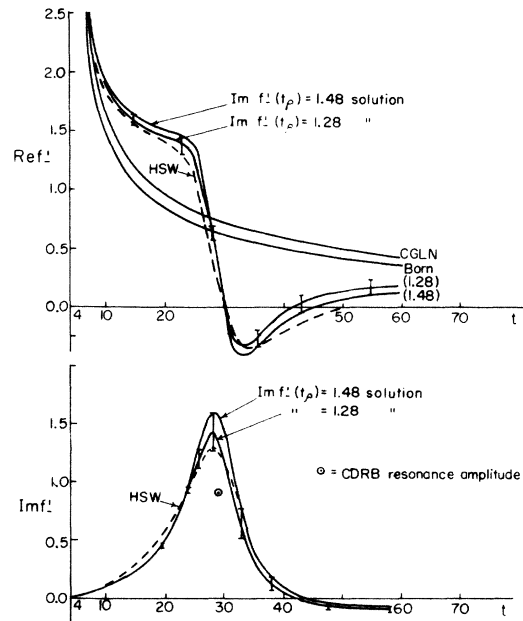
$$\text{Im}\tilde{f}_-^1(t_\rho) = 1.48, \quad (7.9)$$

$$\text{Im}\tilde{\Gamma}_2(t_\rho) = -0.051,$$

which are in fact the respective upper limits as indicated in (7.8). This choice is particularly useful for determining limits of uncertainty in NN potential calculations.⁸ We show the resulting amplitudes and error bands in Figs. 6 and 7. We have also plotted in Fig. 6 a solution for f_-^1 using as input the value

$$\text{Im}\tilde{f}_-^1(t_\rho) = 1.28, \quad (7.10)$$

We note the fact that as for $F_\pi(t)$ the imaginary parts of the amplitude peak at $t \sim 29$, i.e., a little below resonance. In addition, we observe that all the amplitudes go through a zero shortly after $t = 40$. For comparison we have also drawn in the

FIG. 6. The f_-^1 amplitude.

HSW results together with the CGLN⁸ and Born amplitudes. For convenience we have characterized the $J=1$ amplitudes used in the NN calculations of Chemtob, Durso and Riska,⁷ Chemtob and Riska³¹ and Durso and Brown³⁰ (collectively CDRB) by their values at resonance, i.e.,

$$\begin{aligned} \text{Im}\tilde{f}_-^1(t_\rho)|_{\text{CDRB}} &= 0.93, \\ \text{Im}\tilde{\Gamma}_2(t_\rho)|_{\text{CDRB}} &= -0.038. \end{aligned} \quad (7.11)$$

We observe that these fall outside the allowed band of solutions. We also note that the Born terms are large for both amplitudes and, as for f_+^0 , are responsible for the rapid amplitude variations near $t=4$. An interesting feature brought out by a comparison of the CGLN curves for f_+^0 and f_-^1 , Γ_2 is that the $\Delta(1236)$ contribution certainly drops off as we go to higher $N\bar{N} \rightarrow \pi\pi$ helicity amplitudes. This behavior is as predicted by our analysis of the CGLN model which we have described elsewhere.⁸

In summary we can say that our $J=1$ results are similar to previous determinations. It is clear, however, that the amplitudes are not well determined by either our or the other approaches. This is most unfortunate, for when the helicity amplitudes are used to evaluate the $N\bar{N}$ potential, errors in the $J=1$ amplitudes are then amplified consistently.

We now return to the details of the consistency

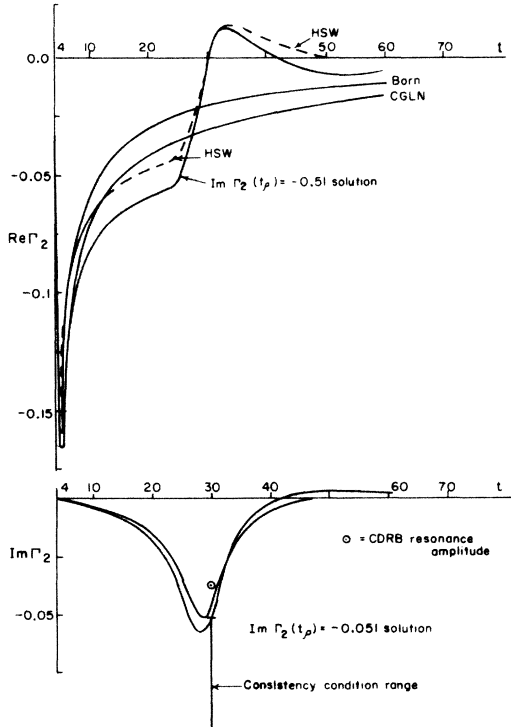


FIG. 7. The Γ_2 amplitude.

condition restrictions on the resonance amplitudes. We illustrate the procedure for \tilde{f}_-^1 . From Sec. VI we write down the unsubtracted Omnès relation for \tilde{f}_-^1 :

$$\begin{aligned} \tilde{f}_-^1(t) e^{-\mu_1(t)} &= \frac{1}{\pi} \int_{-\infty}^0 dt' \frac{\text{Im}\tilde{f}_-^1(t')}{F_\pi(t')(t'-t-i)} \\ &+ \frac{1}{\pi} \int_4^\infty dt' \frac{f_-^1(t')|_{\text{Born}} \sin\delta_1^1(t')}{|F_\pi(t')(t'-t-i\epsilon)|}. \end{aligned} \quad (7.12)$$

At resonance we find

$$\begin{aligned} \text{Im}\tilde{f}_-^1(t_\rho) &= |F_\pi(t_\rho)| \left[\frac{P}{\pi} \int_4^\infty dt' \frac{f_-^1|_{\text{Born}} \sin\delta_1^1}{|F_\pi(t')(t'-t_\rho)|} \right. \\ &\left. + \frac{1}{\pi} \int_{-\infty}^0 dt' \frac{\text{Im}\tilde{f}_-^1}{F_\pi(t)(t'-t_\rho)} \right]. \end{aligned} \quad (7.13)$$

Thus we want an estimate for the quantity

$$\chi_1(t) = \frac{1}{\pi} \int_{-\infty}^{-26} dt' \frac{\text{Im}\tilde{f}_-^1}{F_\pi(t')(t'-t'i\epsilon)} \quad (7.14)$$

when $t=t_\rho$.

Now we make use of our consistency condition at $t=4$ together with Eq. (7.12) and find

$$\chi_1(4) = 0.13. \quad (7.15)$$

Next we assume $\text{Im}\tilde{f}_-^1 < 0$ in the range $-\infty < t < -26$. Support for this comes from the Nielsen tables²⁶ and Eq. (7.15). With this assumption and noting that

$$-\frac{30}{56} \frac{1}{t'-4} < \frac{-1}{t'-t_\rho} < \frac{-1}{t'-4}, \quad (7.16)$$

the following inequality applies:

$$\frac{30}{56} \chi_1(4) < \chi_1(t_\rho) < \chi_1(4). \quad (7.17)$$

In conjunction with (7.13), this implies

$$1.07 < \text{Im}\tilde{f}_-^1(t_\rho) < 1.48. \quad (7.18)$$

We have used our curve A (135-MeV width δ_1^1) for $F_\pi(t)$ here. If we use the curve D defined in Sec. III and plotted in Fig. 2, we obtain

$$0.97 < \text{Im}\tilde{f}_-^1(t_\rho) < 1.40. \quad (7.19)$$

For Γ_2 we define

$$\chi_2(t) = \frac{1}{\pi} \int_{-\infty}^{-26} dt' \frac{\text{Im}\tilde{\Gamma}_2}{F_\pi(t')(t'-t-i\epsilon)}, \quad (7.20)$$

and find

$$\chi_2(4) = -0.013. \quad (7.21)$$

We assume $\text{Im}\tilde{\Gamma}_2 > 0$ in the range $-\infty < t < -26$, with support coming from (7.21) and the Nielsen tables,²⁶ and find

$$\text{Choice A: } -0.1 < \text{Im}\tilde{\Gamma}_2(t_\rho) < -0.056, \quad (7.22)$$

Choice B: $-0.09 < \text{Im}\tilde{\Gamma}_2(t_\rho) < -0.051$.

We should point out that we have used the Nielsen values for $\text{Im}\tilde{f}_-^1$, $\text{Im}\tilde{\Gamma}_2$ in the range $-26 < t < 0$ with no allowance made for errors. We shall return to this shortly. We remark that we have tried a once-subtracted version of this consistency condition scheme and find it leads to wider limits on the amplitudes.

Of course, at this stage one is tempted to fix tighter inequalities by trying an extrapolation of $\chi_1(t)$, $\chi_2(t)$ to $t=t_\rho$. To see if this will work we have evaluated these functions in the range $-25 < t < 3$ using Eqs. (7.12) and its $\tilde{\Gamma}_2$ counterpart, together with the Nielsen tables.²⁹ To obtain some idea of the errors we have carried out the evaluation for both curves A and D for $F_\pi(t)$. The results are plotted in Fig. 8. It is clear that even assuming exact accuracy for the Nielsen input the uncertainty in $F_\pi(t)$ precludes in accurate extrapolation. For this reason we make no attempt to extrapolate to the resonance region. NO made a more detailed analysis of the extrapolation problem. Using as input a δ_1^1 phase shift of width 125 MeV, they obtained

$$\text{Im}\tilde{f}_-^1(t_\rho) = 1.28 \pm 0.13, \quad (7.23)$$

$$\text{Im}\tilde{\Gamma}_2(t_\rho) = -0.056 \pm 0.011.$$

(They actually worked out f_\pm^1 .) The errors quoted reflect only the uncertainty in the πN input data. Thus no allowance is made for errors in $F_\pi(t)$.

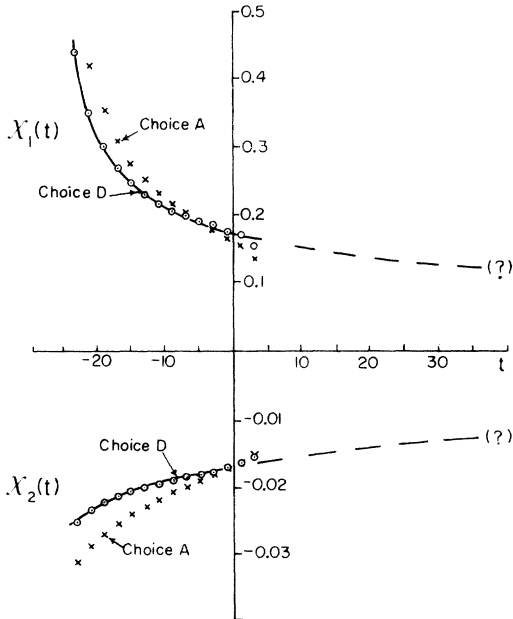


FIG. 8. Plot of $\chi_1(t)$, $\chi_2(t)$ indicating extrapolation hazards.

These results are consistent with our limits.

It is clear from the above that there is quite some latitude in the choice of resonance subtraction constants. The "hard" consistency condition limits are

$$\begin{aligned} 0.97 < \text{Im}\tilde{f}_-^1(t_\rho) < 1.48, \\ 0.1 < \text{Im}\tilde{\Gamma}_2(t_\rho) < -0.051. \end{aligned} \quad (7.24)$$

VIII. CONCLUSIONS

We have successfully applied our consistency conditions in two ways: first as a check on previous helicity-amplitude calculations, where we find the f_+^0 amplitude to be poorly determined by NPP,³ and second as a constraint in Omnès dispersion relations to accurately determine both the entire f_+^0 amplitude and the entire p -wave amplitudes f_-^1 , Γ_2 . In addition we have shown the efficacy of using non-Born Omnès dispersion relations for determining helicity amplitudes.

In summary we can say with confidence that f_+^0 is well determined in our approach, however, our analysis indicates that f_-^1 , Γ_2 are not as well known as has been previously assumed. We describe elsewhere the application of our helicity amplitudes to the problem of calculating the intermediate-range nucleon-nucleon potential.

APPENDIX A

We give here the parametrizations for δ_0^0 , δ_1^1 . δ_0^0 : In the range $4 < t < 40$ we used

$$\delta_0^0(q) = a_0 q + a_1 q^3 + a_2 q^5 + a_3 q^7 + a_4 q^9 + a_5 q^{11}, \quad (A1)$$

where

$$\begin{aligned} a_0 &= 0.20, \\ a_1 &= 0.142\ 362\ 6, \\ a_2 &= 0.003\ 034\ 2, \\ a_3 &= -0.006\ 821\ 0, \\ a_4 &= +0.000\ 896\ 2, \\ a_5 &= -0.000\ 035\ 8. \end{aligned} \quad (A2)$$

An alternative effective range form is that of Brehm, Golowich, and Prasad,³⁵ which (after corrections for misprints) is

$$\begin{aligned} \frac{q}{2(1+q^2)^{1/2}} \cot \delta_0^0 &= \frac{1}{2a_0(1+q^2)} - \frac{1}{2\pi} \frac{q^2}{1+q^2} \ln \Lambda \\ &+ \frac{q}{\pi(1+q^2)^{1/2}} \ln [q + (1+q^2)^{1/2}], \end{aligned} \quad (A3)$$

where $\Lambda = 350$.

Above $t=40$ we dropped δ_0^0 linearly (in q) to zero at $t=200$. Strictly speaking, δ_0^0 should rise rapidly through $\frac{1}{2}\pi$ near $t=51$ and level off on reaching π as indicated by the latest data. However, this "tail" behavior has little effect on our f_+^0 solution except, say, for $t>50$. Thus our f_+^0 results are certainly reliable up to $t=40$, where cutoff independence sets in for the associated NN potential components.

δ_1^1 : We use the Morgan and Shaw-type parametrization¹⁶

$$\left(\frac{q^2}{q^2+1}\right)^{1/2} \cot\delta_1^1 = \frac{(1-0.1536q^2)(1+0.014q^2)}{0.035q^2},$$

for $4 < t < 100$ (A4)

and

$$\delta_1^1 = \pi, \text{ for } t > 100.$$

The effect of this tail on $F_\pi(t)$ is easily evaluated. Recall that

$$\mu_1(t) = \frac{t}{\pi} \int_4^\infty dt' \frac{\delta_1^1(t')}{t'(t'-t-i\epsilon)} \quad (\text{A5})$$

and

$$f(t) = e^{\mu_1(t)}. \quad (\text{A6})$$

Now

$$\mu_1(t)|_{\text{tail}} \equiv \frac{t}{\pi} \int_{100}^X dt' \frac{\delta_1^1(t')}{t'(t'-t-i\epsilon)} \quad (\text{A7})$$

so that

$$\begin{aligned} \mathcal{F} &= |e^{\mu_1(t)}|_{\text{tail}}| \\ &= \left(\frac{100}{100-t}\right) \left(\frac{X-t}{X}\right), \end{aligned} \quad (\text{A8})$$

where X is a cutoff. If we do not include the δ_1^1 tail, we find $\mathcal{F}=1$. If we include the tail according to (A4), then

$$\mathcal{F} = \left(\frac{100}{100-t}\right). \quad (\text{A9})$$

Thus we see inclusion of the tail affects $F_\pi(t)$ considerably at resonance. Our parametrization (A4) is justified by the good fit for $F_\pi(t)$.

APPENDIX B

We derive our dispersion relation for f_+^0 here. To simplify the notation we write

$$F(t) = e^{\mu_0(t)} f_+^0(t) \quad (\text{B1})$$

and derive a dispersion relation for $F(t)/t^2$. The contour around which we apply Cauchy's theorem is shown in Fig. 9. There is a double pole situated on the cut at $t=0$. This must be dealt with carefully, so we split off the piece of the contour near the origin, as illustrated in Fig. 10.

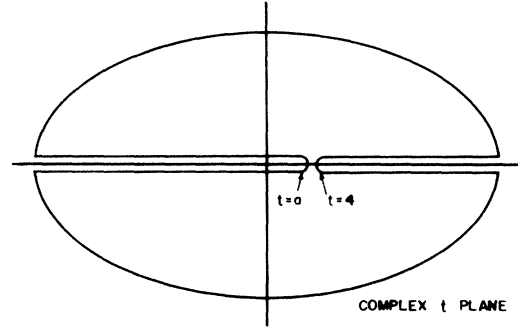


FIG. 9. The integration contour for $F(t)/t^2$ in the complex t plane.

Thus our dispersion relation is

$$\begin{aligned} F(t)/t^2 &= \frac{1}{\pi} \left(\int_h^a + \int_{-\infty}^{-h} \right) \frac{\text{Im}F(t')dt'}{(t')^2(t'-t-i\epsilon)} \\ &+ \frac{1}{\pi} \int_4^\infty \frac{\text{Im}F(t')dt'}{(t')^2(t'-t-i\epsilon)} \\ &+ \text{near-pole contribution.} \end{aligned} \quad (\text{B2})$$

Near-Pole Contribution. Write

$$g = (I_1 + I_2)/2\pi i, \quad (\text{B3})$$

where

$$I_1 = \int_{-h+i\epsilon}^{h+i\epsilon} \frac{F(t')dt'}{(t')^2(t'-t)}, \quad (\text{B4a})$$

$$I_2 = \int_{-h-i\epsilon}^{h-i\epsilon} \frac{F(t')dt'}{(t')^2(t'-t)}. \quad (\text{B4b})$$

Note that $t > 4$ so we have dropped the $i\epsilon$ in the LH-cut integrals. Next we use partial fractions:

$$\frac{1}{(t')^2(t'-t)} = \frac{1}{t^2(t'-t)} - \frac{1}{t^2 t'} - \frac{1}{t(t')^2}, \quad (\text{B5})$$

and write

$$I_1 = I_1^1 + I_1^2 + I_1^3. \quad (\text{B6})$$

Then

$$\begin{aligned} I_1^1 &= \frac{1}{t^2} \int_{-h+i\epsilon}^{h+i\epsilon} \frac{F(t')dt'}{t'-t} \\ &= \frac{1}{t^2} \int_{-h}^h \frac{F(t'+i\epsilon)dt'}{t'-t+i\epsilon}. \end{aligned} \quad (\text{B7})$$

Now we make a Taylor expansion,

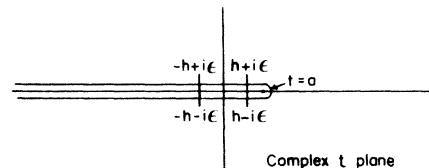


FIG. 10. The region of the contour near $t=0$.

$$F(t' + i\epsilon) = F(i\epsilon) + t'F'(i\epsilon) + \frac{t'^2}{2!}F''(i\epsilon) + \dots \quad (\text{B8})$$

Hence

$$I_1^1 = \frac{1}{t^2} \left[F(i\epsilon) \ln \left(\frac{t+h}{t-h} \right) + 2hF'(i\epsilon) + (t-i\epsilon)F'(i\epsilon) \ln \left(\frac{t+h}{t-h} \right) + \dots \right], \quad (\text{B9})$$

i.e., $I_1^1 = O(h)$. Similarly we find

$$I_1^2 = \frac{i\pi}{t^2} F(i\epsilon) + O(h), \quad (\text{B10})$$

$$I_1^3 = \frac{i\pi}{t} F'(i\epsilon) - \frac{1}{t} \int_{-h}^h \frac{F(i\epsilon) dt'}{(t'+i\epsilon)} + O(h) \\ = \frac{i\pi}{t} F'(i\epsilon) + \frac{1}{t} \frac{2hF'(i\epsilon)}{h^2 + \epsilon^2} + O(h). \quad (\text{B11})$$

In the above we have made use of the integrals

$$U_1 = \int_{-h}^h \frac{dt'}{t'+i\epsilon} = -i\pi, \\ U_2 = \int_{-h}^h \frac{dt'}{(t'+i\epsilon)^2} = -\frac{2h}{h^2 + \epsilon^2}, \\ U_3 = \int_{-h}^h \frac{t' dt'}{(t'+i\epsilon)^2} = -i\pi + \frac{2ih\epsilon}{h^2 + \epsilon^2}, \\ U_4 = \int_{-h}^h \frac{(t')^2 dt'}{(t'+i\epsilon)^2} = 2h - 2\epsilon\pi + \frac{2h\epsilon^2}{h^2 + \epsilon^2}. \quad (\text{B12})$$

Hence we find

$$g = \frac{1}{t^2} \operatorname{Re}F(0) + \frac{1}{t} \operatorname{Re}F'(0) + \frac{1}{\pi} \frac{2h \operatorname{Im}F(i\epsilon)}{t(h^2 + \epsilon^2)}. \quad (\text{B13})$$

Thus, neglecting the RH cut we have

$$\frac{F(t)}{t^2} = \frac{1}{\pi} \left(\int_h^a + \int_{-\infty}^{-h} \right) \frac{\operatorname{Im}F(t') dt'}{(t')^2(t'-t)} + \frac{1}{t^2} \operatorname{Re}F(0) \\ + \frac{1}{t} \operatorname{Re}F'(0) + \frac{1}{\pi t} \frac{2 \operatorname{Im}F(0)}{h} + O(h). \quad (\text{B14})$$

Now what happens as $h \rightarrow 0$? Write $F(t) = F(t, h) = G(h)$ so that for $h_1 > h_2 > 0$ we get

$$G(h_2) - G(h_1) = \frac{1}{\pi} \left(\int_{h_2}^{h_1} + \int_{-h_1}^{-h_2} \right) \frac{\operatorname{Im}F(t') dt'}{(t')^2(t'-t)} \\ + \frac{2 \operatorname{Im}F(0)}{\pi t} \left(\frac{1}{h_2} - \frac{1}{h_1} \right) + O(h_1, h_2). \quad (\text{B15})$$

Now for h_1, h_2 small enough we can replace

$$\frac{\operatorname{Im}F(t')}{t'-t}$$

by

$$-\frac{\operatorname{Im}F(0)}{t}.$$

Hence

$$G(h_2) - G(h_1) = -\frac{1}{\pi t} \left(\int_{h_2}^{h_1} + \int_{-h_1}^{-h_2} \right) \frac{\operatorname{Im}F(0) dt'}{(t')^2} \\ + \frac{2 \operatorname{Im}F(0)}{\pi t} \left(\frac{1}{h_2} - \frac{1}{h_1} \right) + O(h_1, h_2) \\ = O(h_1, h_2). \quad (\text{B16})$$

Hence as $h \rightarrow 0$, $F(t)/t^2$ approaches a definite limit. For computational purposes it is necessary to get the dispersion relation into a form without the explicit limit $h \rightarrow 0$. Thus we now consider the terms in the dispersion relation dependent on h . Write

$$\chi(t) = \frac{1}{\pi} \left(\int_h^a + \int_{-2\epsilon}^{-h} \right) \frac{\operatorname{Im}F(t') dt'}{(t')^2(t'-t)} \\ + \frac{1}{\pi t} \frac{2 \operatorname{Im}F(i\epsilon)}{h}, \quad (\text{B17})$$

where we have now introduced the cutoff at $t = -2\epsilon$. Now we write

$$\chi(t) = \frac{1}{\pi} \int_{-2\epsilon}^a \frac{\operatorname{Im}[F(t') - F(0) - t'F'(0)] dt'}{(t')^2(t'-t)} \\ - \frac{1}{\pi} \int_{-h}^h \frac{\operatorname{Im}[F(t') - F(0) - t'F'(0)] dt'}{(t')^2(t'-t)} \\ + \frac{1}{\pi} \left(\int_h^a + \int_{-2\epsilon}^{-h} \right) \frac{\operatorname{Im}F'(0) dt'}{t'(t'-t)} + H(t), \quad (\text{B18})$$

where

$$H(t) = \frac{1}{\pi} \left(\int_h^a + \int_{-2\epsilon}^{-h} \right) \frac{\operatorname{Im}F(0) dt'}{(t')^2(t'-t)} \\ + \frac{1}{\pi t} \frac{2 \operatorname{Im}F(0)}{h}. \quad (\text{B19})$$

After some manipulation we find

$$\chi(t) = \frac{1}{\pi} \int_{-2\epsilon}^a \frac{\operatorname{Im}[F(t') - F(0) - t'F'(0)] dt'}{(t')^2(t'-t)} \\ + \frac{\operatorname{Im}F(0)}{\pi} \left\{ \frac{1}{t^2} \ln \left[\frac{26(t-a)}{a(t+26)} \right] + \frac{1}{t} \left(\frac{1}{a} + \frac{1}{26} \right) \right\} \\ + \frac{\operatorname{Im}F'(0)}{\pi t} \left[\ln \frac{26(t-a)}{a(t+26)} \right], \quad (\text{B20})$$

and our final dispersion relation reads

$$\begin{aligned}
e^{-\mu_0(t)}f_+^0(t) &= \text{Re}f_+^0(0) + t \left(\text{Re} \frac{\partial}{\partial t} [e^{-\mu_0(t)}f_+^0(t)] \right)_{t=0} + \frac{\text{Im}f_+^0(0)}{\pi} \left\{ \ln \left[\frac{26(t-a)}{a(t+26)} \right] + t \left(\frac{1}{a} + \frac{1}{26} \right) \right\} \\
&+ \frac{t}{\pi} \left(\text{Im} \frac{\partial}{\partial t} [e^{-\mu_0(t)}f_+^0(t)] \right)_{t=0} \ln \left[\frac{26(t-a)}{a(t+26)} \right] \\
&+ \frac{t}{\pi} \int_{-26}^a dt' \frac{e^{-\mu_0(t')} \text{Im}f_+^0(t') - \text{Im}f_+^0(0) - t' \{ \text{Im}(\partial/\partial t'') [e^{-\mu_0(t'')}f_+^0(t'')] \}_{t''=0}}{(t')^2(t'-t)}, \quad \text{for } t > 4. \quad (\text{B21})
\end{aligned}$$

APPENDIX C

We demonstrate the rapid variations of $\text{Im}f_-^1(t)|_{\text{Born}}$ near $t=a$. From Frazer and Fulco¹⁰ or Eqs. (2.2) and (2.3) we write

$$\text{Im}f_-^1(t)|_{\text{Born}} = \frac{\sqrt{2}g^2}{16p_-q_-} \left[\frac{(\frac{1}{2}t-1)^2}{4(p_-q_-)^2} - 1 \right], \quad (\text{C1})$$

where

$$\begin{aligned}
p_- &= (m - \frac{1}{4}t)^{1/2}, \\
q_- &= (1 - \frac{1}{4}t)^{1/2}.
\end{aligned} \quad (\text{C2})$$

Now when $t=a=4(1-1/4m^2)$, then

$$\begin{aligned}
q_- &= \frac{1}{2m}, \\
p_- &= \frac{2m^2-1}{2m}
\end{aligned} \quad (\text{C3})$$

so that

$$z_0 \equiv \frac{\frac{1}{2}t-1}{2p_-q_-} = 1, \quad (\text{C4})$$

i.e.,

$$\text{Im}f_-^1(a)|_{\text{Born}} = 0. \quad (\text{C5})$$

Thus we must look in the neighborhood of $t=a$.

We set

$$t = a - \delta, \quad (\text{C6})$$

where δ is very small. Then

$$q_- \simeq \frac{1}{2m} (1 + \frac{1}{2}m^2\delta) \quad (\text{C7})$$

and

$$p_- \simeq \frac{2m^2-1}{2m} \left[1 + \frac{m^2\delta}{2(2m^2-1)^2} \right], \quad (\text{C8})$$

which leads to

$$z_0 = 1 - \frac{2m^6\delta}{(2m^2-1)^2}. \quad (\text{C9})$$

Hence

$$\begin{aligned}
\text{Im}f_-^1(a-\delta)|_{\text{Born}} &\simeq \left(\frac{1}{16}\sqrt{2}g^2 \right) 2m^4\delta \\
&\simeq 6.4 \times 10^4 \delta.
\end{aligned} \quad (\text{C10})$$

Thus it is clear that there are rapid variations in $\text{Im}f_-^1|_{\text{Born}}$ near $t=a$.

Of course it is natural to enquire as to the situation for Γ_2 and also f_+^0 . We find

$$\text{Im}\Gamma_2(a-\delta)|_{\text{Born}} \simeq \frac{g^2}{8m}, \quad (\text{C11})$$

$$\text{Im}f_+^0(a-\delta)|_{\text{Born}} \simeq -\left(\frac{1}{8}mg^2\right).$$

Hence there are no sudden variations in either Γ_2 or f_+^0 .

¹G. Höhler, R. Strauss, and H. Wunder, Karlsruhe report, 1968 (unpublished) (referred to as HSW).

²H. Nielsen and G. C. Oades, Nucl. Phys. **B49**, 586 (1972) (referred to as NO).

³H. Nielsen, J. Lyng Petersen, and E. Pietarinen, Nucl. Phys. **B22**, 525 (1970) (referred to as NPP).

⁴H. B. Geddés and R. H. Graham, Phys. Rev. D **7**, 1801 (1973).

⁵D. Amati, E. Leader and B. Vitale, Phys. Rev. **130**, 750 (1963).

⁶W. N. Cottingham and R. Vinh Mau, Phys. Rev. **130**, 735 (1963).

⁷M. Chemtob, J. W. Durso, and D. O. Riska, Nucl. Phys. **B38**, 232 (1972).

⁸G. N. Epstein and B. H. J. McKellar, Bull. Am. Phys. Soc. **16**, 1150 (1971); Nuovo Cimento Lett. **5**, 807 (1972); Phys. Rev. D **10**, 1005 (1974).

⁹G. N. Epstein and B. H. J. McKellar, Nuovo Cimento Lett. **8**, 177 (1973).

¹⁰W. R. Frazer and J. R. Fulco, Phys. Rev. **117**, 1603 (1960).

¹¹S. M. Flatté *et al.*, Phys. Lett. **38B**, 232 (1972).

¹²J. D. Jackson, Rev. Mod. Phys. **42**, 12 (1970).

¹³D. Morgan and J. Pišút, in *Springer Tracts in Modern Physics*, edited by G. Höhler (Springer, New York, 1970), Vol. 55.

¹⁴J. L. Petersen, Phys. Rep. **C2**, 155 (1971).

¹⁵J. L. Basdevant, C. D. Froggatt, and J. L. Petersen, Phys. Lett. **41B**, 173 (1972); **41B**, 178 (1972).

¹⁶D. Morgan and G. Shaw, Phys. Rev. D **2**, 520 (1970).

¹⁷S. Weinberg, Phys. Rev. Lett. **17**, 616 (1966).

¹⁸C. W. Akerlof, W. W. Ash, K. Berkelman, C. A. Lichtenstein, A. Ramanauskas, and R. H. Siemann, Phys. Rev. **163**, 1482 (1967).

- ¹⁹C. Mistretta, J. A. Appel, R. J. Budnitz, L. Carroll, J. Chen, J. R. Dunning, Jr., M. Goitein, K. Hanson, D. C. Imrie, and R. Wilson, *Phys. Rev.* **184**, 1487 (1969).
- ²⁰C. N. Brown, C. R. Canizares, W. E. Cooper, A. M. Eisner, G. J. Feldman, C. A. Lichtenstein, L. Litt, W. Lockeretz, V. B. Montana, and F. M. Pipkin, *Phys. Rev. Lett.* **26**, 991 (1971).
- ²¹V. L. Auslender, G. I. Budker, E. V. Pakhtusova, Yu N. Pestov, V. A. Sidorov, A. N. Skrinskii, and A. G. Khabakhpashev, *Yad. Fiz.* **9**, 114 (1969) [*Sov. J. Nucl. Phys.* **9**, 69 (1969)].
- ²²D. Benaksas, G. Cosme, B. Jean-Marie, S. Julian, F. Laplanche, J. Lefrançois, A. D. Liberman, G. Parrour, J. P. Repellin, and G. Sauvage, *Phys. Lett.* **39B**, 289 (1972).
- ²³M. Roos and J. Pišút, *Nucl. Phys.* **B10**, 563 (1969).
- ²⁴J. Engels, *Nucl. Phys.* **B36**, 73 (1972).
- ²⁵G. Höhler and R. Strauss, *Z. Phys.* **232**, 205 (1970).
- ²⁶H. Nielsen, *Nucl. Phys.* **B33**, 152 (1971).
- ²⁷J. Hamilton, P. Menotti, G. C. Oades, and L. L. J. Vick, *Phys. Rev.* **128**, 1881 (1962).
- ²⁸P. Menotti, *Nuovo Cimento* **23**, 931 (1962).
- ²⁹S. Furuichi and K. Watanabe, *Prog. Theor. Phys.* **37**, 465 (1967).
- ³⁰G. E. Brown and J. W. Durso, *Phys. Lett.* **35B**, 120 (1971).
- ³¹M. Chemtob and D. O. Riska, *Phys. Lett.* **35B**, 115 (1971).
- ³²P. D. Kapadia, *Nucl. Phys.* **B3**, 291 (1967).
- ³³L. L. J. Vick, *Nuovo Cimento* **31**, 643 (1964).
- ³⁴G. J. Gounaris and J. J. Sakurai, *Phys. Rev. Lett.* **21**, 244 (1968).
- ³⁵J. J. Brehm, E. Golowich, and S. C. Prasad, *Phys. Rev. Lett.* **25**, 67 (1970).